

# A Comparison of Cosmological Models Using Time Delay Lenses

Jun-Jie Wei<sup>1,2</sup>, Xue-Feng Wu<sup>1,3,4</sup>, and Fulvio Melia<sup>5</sup>

Received \_\_\_\_\_; accepted \_\_\_\_\_

---

<sup>1</sup>Purple Mountain Observatory, Chinese Academy of Sciences, Nanjing 210008, China; jjwei@pmo.ac.cn, xfwu@pmo.ac.cn.

<sup>2</sup>University of Chinese Academy of Sciences, Beijing 100049, China

<sup>3</sup>Chinese Center for Antarctic Astronomy, Nanjing 210008, China.

<sup>4</sup>Joint Center for Particle, Nuclear Physics and Cosmology, Nanjing University-Purple Mountain Observatory, Nanjing 210008, China.

<sup>5</sup>Department of Physics, The Applied Math Program, and Department of Astronomy, The University of Arizona, AZ 85721, USA; fmelia@email.arizona.edu.

## ABSTRACT

The use of time-delay gravitational lenses to examine the cosmological expansion introduces a new standard ruler with which to test theoretical models. The sample suitable for this kind of work now includes 12 lens systems, which have thus far been used solely for optimizing the parameters of  $\Lambda$ CDM. In this paper, we broaden the base of support for this new, important cosmic probe by using these observations to carry out a one-on-one comparison between *competing* models. The currently available sample indicates a likelihood of  $\sim 70 - 80\%$  that the  $R_h = ct$  Universe is the correct cosmology versus  $\sim 20 - 30\%$  for the standard model. This possibly interesting result reinforces the need to greatly expand the sample of time-delay lenses, e.g., with the successful implementation of the Dark Energy Survey, the VST ATLAS survey, and the Large Synoptic Survey Telescope. In anticipation of a greatly expanded catalog of time-delay lenses identified with these surveys, we have produced synthetic samples to estimate how large they would have to be in order to rule out either model at a  $\sim 99.7\%$  confidence level. We find that if the real cosmology is  $\Lambda$ CDM, a sample of  $\sim 150$  time-delay lenses would be sufficient to rule out  $R_h = ct$  at this level of accuracy, while  $\sim 1,000$  time-delay lenses would be required to rule out  $\Lambda$ CDM if the real Universe is instead  $R_h = ct$ . This difference in required sample size reflects the greater number of free parameters available to fit the data with  $\Lambda$ CDM.

*Subject headings:* cosmology: observations, theory; gravitational lensing: strong; galaxies: halos, structure; quasars: general

## 1. Introduction

The idea of using gravitational lenses with time delays between the various images of a background quasar as a cosmological probe was first suggested by Refsdal (1964). Null geodesics originating with distant variable sources have different optical paths and pass through dissimilar gravitational potentials. Their deflection angles and time delays can thus be used to infer lens-system dependent angular-diameter distances, which can then be compared to theoretical predictions from general relativity to test the background cosmological expansion and offer the possibility of testing competing models (see, e.g., Petters et al. 2001; Schneider et al. 2006).

As of today, time delays have been observed from 21 lensed quasars, a relatively small subset of the several hundred known strong-lens systems. But this is only the beginning. In the near future, observational programmes, such as the COSmological MONitoring of GRAvItational Lenses (COSMOGRAIL; Eigenbrod et al. 2005) and perhaps also the International Liquid Mirror Telescope (ILMT) project (Jean et al. 2001), which is now in the final phases of construction in the Kumaun region of the Himalayas (Sagar et al. 2013), should increase this sample considerably. New strong gravitational lens systems will also be discovered by cosmic structure surveys, including the Dark Energy Survey<sup>1</sup>

---

<sup>1</sup>One should take note of the fact, however, that the actual image quality in these surveys may be inferior to that expected, somewhat mitigating the possible yield of suitable lens systems for this work. For example, the DES was aiming to get 0.9'' median FWHM in the r, i, and z band images for its wide survey. At the end of the first year, the quality is close to this, though not yet meeting expectations. In addition, g and Y bands are observed in poorer seeing conditions so their quality is even lower (Bernstein 2014). This is an important consideration in any discussion concerning anticipated sample size, given that even SDSS has discovered only  $\sim 5\%$  of the originally expected lens systems.

(DES; Banerji et al. 2008; Buckley-Geer et al. 2014; Schneider 2014), the Large Synoptic Survey Telescope (LSST; Tyson et al. 2002; Blandford et al. 2006; Marshall et al. 2011; Chang et al. 2014) project, and the VST ATLAS survey (Koposov et al. 2014), and time delays will be measured for a sub-sample of these with subsequent monitoring observations. Oguri & Marshall (2010) carried out a detailed calculation of the likely yields of several planned surveys, using realistic distributions for the lens and source properties and taking magnification bias and image configuration detectability into account. They found that upcoming wide-field synoptic surveys should detect several thousand lensed quasars. In particular, LSST should find more than  $\sim 8,000$  lensed quasars, some 3,000 of which will have well-measured time delays.

Several attempts have already been made to demonstrate the usefulness of these data for constraining the cosmological parameters in the standard model,  $\Lambda$ CDM (see, e.g., Paraficz & Hjorth 2009, 2010; Balmès & Corasaniti 2013; and Suyu et al. 2013). In this paper, we broaden the base of support for this cosmic probe by demonstrating its usefulness in testing *competing* cosmological models. In particular, we show that the currently available sample of time-delay lensing systems favors the  $R_h = ct$  Universe with a likelihood of  $\sim 70 - 80\%$  of being correct, versus  $\sim 20 - 30\%$  for  $\Lambda$ CDM. Though this result is still only marginal, it nonetheless calls for a significant increase in the sample of suitable lensing systems in order to carry out more sophisticated and higher precision measurements.

In § 2, we describe the key theoretical steps used in the application of time-delay lenses for cosmological testing, and we apply this procedure to the currently known sample of 12 systems in § 3. We discuss the results of our one-on-one comparison between  $\Lambda$ CDM and  $R_h = ct$  in § 4. As we shall see, model selection tools favor the latter, but the distinction, given the relatively small number of lenses, is still not strong enough to completely rule out either model. We therefore estimate the sample size required from future surveys to

reach likelihoods of  $\sim 99.7\%$  and  $\sim 0.3\%$ , for a  $3\sigma$  confidence limit, and we present our conclusions in § 6.

## 2. Strong Lensing

The measurement of time delays in strong gravitational lenses is not straightforward, due in part to the uncertainty associated with the lens mass distribution and the possible presence of other perturbing masses along the line-of-sight. To this point, two principal methods have been employed to model the lens itself, which may be characterized as either simple-parametric (see, e.g., Oguri et al. 2002; Keeton et al. 2003) or grid-based parametric (see, e.g., Warren & Dye 2003; Bradac et al. 2008; Coles 2008; Suyu et al. 2013) approaches. The former uses simply-parametrized forms for the mass distribution of the deflector, while the latter uses as parameters a grid of pixels, to describe either the potential or the mass distribution of the deflector, and/or the source surface brightness distribution. Some have also used a hybrid approach, in which pixellated corrections were made to a simply parametrized mass model (Suyu et al. 2010; Vegetti et al. 2010).

The grid-based methods are regularized, often by imposing physical priors, otherwise they would just fit the noise. The simply parametrized methods can even be computationally more intensive, depending on the choice of the parameters. If an appropriate sub-sample of homogeneous systems can be identified—meaning a set of lenses whose properties provide evidence that the same lens model description may be used with the same level of statistical significance—the simply parametrized method can serve as an ideal first attempt at gauging whether the image-inversion effort is warranted with follow-up analysis. This is the method we will be using in this paper.

For a given image  $i$  at angular position  $\vec{\theta}_i$ , with the source position at angle  $\vec{\beta}$ , the time

delay,  $\Delta t_i$ , is the combined effect of the difference in path length between the straight and deflected rays, and the gravitational time dilation for the ray passing through the effective gravitational potential of the lens,  $\Psi(\vec{\theta}_i)$ :

$$\Delta t_i = \frac{1 + z_l}{c} \frac{D_A(0, z_s) D_A(0, z_l)}{D_A(z_l, z_s)} \left[ \frac{1}{2} (\vec{\theta}_i - \vec{\beta})^2 - \Psi(\vec{\theta}_i) \right] \quad (1)$$

(see, e.g., Blandford & Narayan 1986, and references cited therein), where  $z_l$  and  $z_s$  are the lens and source redshifts, respectively, and  $D_A(z_1, z_2)$  is the angular-diameter distance between redshifts  $z_1$  and  $z_2$ . If the lens geometry  $\vec{\theta}_i - \vec{\beta}$  and the lens potential  $\Psi$  are known, the time delay measures the ratio

$$\mathcal{R} \equiv \frac{D_A(0, z_s) D_A(0, z_l)}{D_A(z_l, z_s)}, \quad (2)$$

also known as the time-delay distance, which depends on the cosmological model.

It has been known for over a decade that lens spiral and elliptical galaxies have a mass distribution that is well approximated by power-law density profiles (Witt et al. 2000; Rusin et al. 2003), for which the lens potential may be written

$$\Psi(\vec{\theta}) = \frac{b^2}{3 - n} \left( \frac{\theta}{b} \right)^{3-n}, \quad (3)$$

in terms of the deflection scale  $b$  and index  $n$ . The single isothermal sphere (SIS) is the special case corresponding to  $n = 2$ , for which  $b = 4\pi D_A(z_l, z_s) \sigma_\star^2 / D_A(0, z_s)$ , where  $\sigma_\star$  is the velocity dispersion of the lensing galaxy. Though some systems have shallow profiles with  $n < 1$ , measurements of galaxy density distributions suggest that  $n$  is generally close to the isothermal value. Thus, in addition to the SIS model being convenient for its simplicity, it is actually also a surprisingly useful and accurate model for lens galaxies (Guimaraes & Sodr  2009; Koopmans et al. 2009). And for such systems with only two images at  $\vec{\theta}_A$  and  $\vec{\theta}_B$ , the time delay is given by the expression

$$\Delta t = t_A - t_B = \frac{1 + z_l}{2c} \mathcal{R}(z_l, z_s) (\theta_B^2 - \theta_A^2). \quad (4)$$

Treu et al. (2006) found that the ratio  $f \equiv \sigma_*/\sigma_{\text{SIS}}$  is very close to unity, where  $\sigma_{\text{SIS}}$  includes systematic errors in the rms deviation of the velocity dispersion and a softened isothermal sphere potential (see additional details below). Note that if the velocity dispersion  $\sigma_*$  of the lensing galaxy could also be observed, and assuming a ratio  $f = 1$ , two of the angular-diameter distances appearing in equation (2) could be replaced with the measured value of  $\sigma_*$  and the Einstein radius  $\theta_E = (\theta_A + \theta_B)/2$ . An alternative approach would be to impose some prior (see, e.g., Oguri 2007), or to compute  $\sigma_*$  from a dynamical model (see, e.g., Treu & Koopmans 2002). As shown by Paraficz & Hjorth (2009), the quantity  $\Delta t/\sigma_{\text{SIS}}^2$  is more sensitive to the cosmological parameters than  $\Delta t$  or  $\sigma_{\text{SIS}}^2$  separately, so this additional datum would improve the reliability with which this approach could distinguish between competing models. As of today, however, there are simply too few time-delay lenses with the corresponding measure of  $\sigma_*$ , so all of the analysis we carry out in this paper will be based solely on the use of equation (4). Even looking to the future, velocity dispersions are particularly difficult to measure for these systems precisely because they are crowded by quasars that make the time delay measurement possible.

In  $\Lambda$ CDM, the angular-diameter distance depends on several parameters, including  $H_0$  and the mass fractions  $\Omega_m \equiv \rho_m/\rho_c$ ,  $\Omega_r \equiv \rho_r/\rho_c$ , and  $\Omega_{\text{de}} \equiv \rho_{\text{de}}/\rho_c$ , defined in terms of the current matter ( $\rho_m$ ), radiation ( $\rho_r$ ), and dark energy ( $\rho_{\text{de}}$ ) densities, and the critical density  $\rho_c \equiv 3c^2 H_0^2/8\pi G$ . Assuming zero spatial curvature, so that  $\Omega_m + \Omega_r + \Omega_{\text{de}} = 1$ , the angular-diameter distance between redshifts  $z_1$  and  $z_2$  ( $> z_1$ ) is given by the expression

$$D_A^{\Lambda\text{CDM}}(z_1, z_2) = \frac{c}{H_0} \frac{1}{(1+z_2)} \int_{z_1}^{z_2} [\Omega_m(1+z)^3 + \Omega_r(1+z)^4 + \Omega_{\text{de}}(1+z)^{3(1+w_{\text{de}})}]^{-1/2} dz, \quad (5)$$

where  $p_{\text{de}} = w_{\text{de}}\rho_{\text{de}}$  is the dark-energy equation of state. Thus, the essential free parameters in flat  $\Lambda$ CDM are  $H_0$ ,  $\Omega_m$  and  $w_{\text{de}}$  (since radiation is insignificant at gravitational lensing redshifts). In the  $R_h = ct$  Universe (Melia 2007; Melia & Shevchuk 2012), the

angular-diameter distance depends only on  $H_0$ . In this cosmology,

$$D_A^{R_h=ct}(z_1, z_2) = \frac{c}{H_0} \frac{1}{(1+z_2)} \ln \left( \frac{1+z_2}{1+z_1} \right). \quad (6)$$

### 3. Sample of Time-Delay (Two-image) Lensing Systems

In their careful Bayesian approach to constraining  $H_0$  within the framework of  $\Lambda$ CDM, Balmès & Corasaniti (2013) collected a sample of time-delay lenses for which Bayesian selection techniques can identify the lens mass model with the highest probability of describing the lens system. Rather than attempting to model individual lenses in all their complexity, the goal was to identify the model whose parameters significantly influence the time-delay, allowing them to average over individual mass model parameter uncertainties on a homogeneous mass sample. The first selection criterion in such an approach is therefore a restriction to two-image lenses, listed in Table 1, which seem to be more likely than other lens systems to be consistent with a simple power-law (or even SIS) profile. Paraficz & Hjorth (2010) followed the alternative method of using inversion techniques with each individual intensity image to map the mass distribution in each individual lens system, and produced a very useful comparison of their mass profiles, shown in Figure 1 of that paper. Indeed, the two-image lenses are significantly more symmetric than the rest. But though the object constituting the lens has been identified unambiguously in all the entries listed in Table 1, it is not yet clear whether these are part of a group or whether perturbators contribute along the line-of-sight. Thus, at this stage, an important caveat to our conclusions is that external shear may yet be contributing to some selection bias.

Note, however, that the two-image criterion may not be sufficient to guarantee a simple power-law lens model. Balmès and Corasaniti (2013) concluded from this sample that nine have Bayes factors favoring such a mass profile, though six of these are somewhat inconclusive. Thus, for a more balanced assessment in our analysis, we will consider two



sample cuts, one with the full set of 12 two-image lenses listed in Table 1, and the second with just these nine: B1600+434, SBS 1520+530, SDSS J1650+4251, B0218+357, FBQ 0951+2635, HE 2149-2745, PKS 1830-211, Q0142-100, and SBS 0909+532.

For each model, we find the optimized fit by maximizing the joint likelihood function

$$L(\sigma_{\text{SIS}}, \xi) \propto \prod_{i=1} \frac{1}{\sqrt{\sigma_{\text{SIS}}^2 + \sigma_{\mathcal{R}_i}^2}} \times \exp \left[ -\frac{(\mathcal{R}_{\text{th},i}[\xi] - \mathcal{R}_{\text{obs},i})^2}{2(\sigma_{\text{SIS}}^2 + \sigma_{\mathcal{R}_i}^2)} \right], \quad (7)$$

where ‘th’ stands for either  $\Lambda$ CDM or  $R_{\text{h}} = ct$ ,  $\mathcal{R}_{\text{th}}$  is the theoretical time-delay distance calculated from  $z_{l,i}$ ,  $z_{s,i}$  and the model specific parameters  $\xi$ ,  $\mathcal{R}_{\text{obs}}$  is the measured value, and  $\sigma_{\mathcal{R}}$  is the dispersion of  $\mathcal{R}_{\text{obs}}$ . The measured time-delay distance is

$$\mathcal{R}_{\text{obs}}(z_l, z_s) = \frac{2c}{1 + z_l} \frac{\Delta t}{(\theta_B^2 - \theta_A^2)}, \quad (8)$$

so the propagated error  $\sigma_{\mathcal{R}}$  in  $\mathcal{R}_{\text{obs}}$  is

$$\sigma_{\mathcal{R}} = \mathcal{R}_{\text{obs}} \left[ \left( \frac{\sigma_{\Delta t}}{\Delta t} \right)^2 + 4 \left( \frac{\theta_B \sigma_{\theta_B}}{\theta_B^2 - \theta_A^2} \right)^2 + 4 \left( \frac{\theta_A \sigma_{\theta_A}}{\theta_B^2 - \theta_A^2} \right)^2 \right]^{1/2}. \quad (9)$$

The dispersion  $\sigma_z$  in the measured redshifts  $z_l$  and  $z_s$  (which enter through the angular distances in  $\mathcal{R}_{\text{obs}}$ ) will be ignored here because a careful analysis of SDSS quasar spectra shows that  $\sigma_z/(1+z) \sim 10^{-4}$  (Hewett & Wild 2010), much smaller than the other errors appearing in equation (9).

However, we must include another source of error, in addition to  $\sigma_{\mathcal{R}}$ , that we will call  $\sigma_{\text{SIS}}$ ; this takes into account at least several effects that apparently give rise to the observed scatter of individual lenses about the pure SIS profile. These include: systematic errors in the rms deviation of the velocity dispersion and a softened isothermal sphere potential, which tends to decrease the typical image separations. Moreover, Koopmans et al. (2009) showed that the mean mass density profile is slightly steeper than SIS and has significant scatter, not to mention that the line of sight contribution is generally non-zero on average

(Suyu et al. 2010). According to Cao et al. (2012),  $\sigma_{\text{SIS}}$  may be as big as  $\sim 20\%$ , depending on how many such factors actually contribute to this scatter. In our approach, we will adopt the additional free parameter  $\eta$  to relate the dispersion  $\sigma_{\text{SIS}}$  to the measured effective lensing distance  $\mathcal{R}_{\text{obs}}$ , according to

$$\sigma_{\text{SIS}} \equiv \eta \mathcal{R}_{\text{obs}}. \quad (10)$$

We will add  $\sigma_{\text{SIS}}$  and  $\sigma_{\mathcal{R}}$  in quadrature, and optimize the parameter  $\eta$  for each fit individually though, as we shall see, the value of  $\eta$  appears to be quite independent of the model itself. Thus, the total uncertainty  $\sigma_{\text{tot}}$  in  $\mathcal{R}_{\text{obs}}$  is given by the expression  $\sigma_{\text{tot}}^2 = \sigma_{\text{SIS}}^2 + \sigma_{\mathcal{R}}^2$ .

#### 4. Results and Discussion

We have used the data shown in Table 1 to directly compare  $\Lambda$ CDM with the  $R_{\text{h}} = ct$  Universe. The parameters in each model were individually optimized by maximizing the likelihood estimation, as described above. We will use two well established priors associated with the concordance  $\Lambda$ CDM model: (i) dark energy is a cosmological constant, so  $w_{\text{de}} = -1$ ; and the spatial curvature constant is zero, i.e., the Universe is flat, so that  $\Omega_{\Lambda} = 1 - \Omega_{\text{m}}$ . But to allow for added flexibility in the optimization of the model fit, we will employ three free parameters:  $H_0$ ,  $\Omega_{\text{m}}$ , and  $\eta$ . We have restricted the fraction  $\Omega_{\text{m}}$  to the range  $(0.0, 1.0)$ . With the full sample of 12 time-delay lenses,  $\Lambda$ CDM fits the data with a maximum likelihood for  $H_0 = 87_{-16}^{+17} (1\sigma) \text{ km s}^{-1} \text{ Mpc}^{-1}$ ,  $\Omega_{\text{m}} = 0.48_{-0.37}^{+0.25} (1\sigma)$  and  $\eta = 0.29_{-0.09}^{+0.15} (1\sigma)$ . The best fit with the  $R_{\text{h}} = ct$  Universe has only two free parameters:  $H_0 = 81_{-13}^{+18} (1\sigma) \text{ km s}^{-1} \text{ Mpc}^{-1}$  and  $\eta = 0.29_{-0.09}^{+0.16} (1\sigma)$ . The entries in column 7 of Table 1 are calculated from the observed angles and time delays. By comparison, columns 8 and 9 show the entries for  $\mathcal{R}_{\Lambda\text{CDM}}$  and  $\mathcal{R}_{R_{\text{h}}=ct}$ , respectively, corresponding to these best-fit parameters using all 12 lens systems.

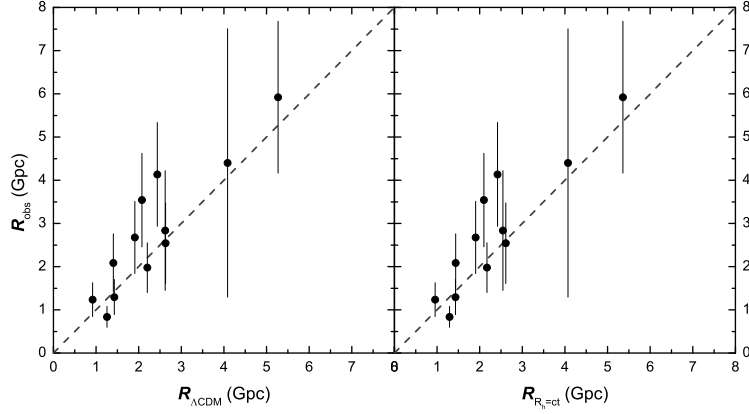


Fig. 1.— Twelve  $\mathcal{R}$  measurements, with error bars, compared to two theoretical models: (*left*) the standard  $\Lambda$ CDM cosmology, assuming a flat universe, with  $H_0 = 87^{+17}_{-16}$  km s $^{-1}$  Mpc $^{-1}$ ,  $\Omega_m = 0.48^{+0.25}_{-0.37}$  and  $\eta = 0.29^{+0.15}_{-0.09}$ ; and (*right*) the  $R_h = ct$  Universe, with  $H_0 = 81^{+18}_{-13}$  km s $^{-1}$  Mpc $^{-1}$  and  $\eta = 0.29^{+0.16}_{-0.09}$ .

To facilitate a direct comparison between  $\Lambda$ CDM and  $R_h = ct$ , we show in Figure 1 the 12 observed values of  $\mathcal{R}_{\text{obs}}$  compared with those predicted by these two theoretical models. The optimized values of  $\eta$  and the maximum likelihood are quite similar for these two cases. However, these models formulate their observables (such as the angular diameter distances in Equations 5 and 6) differently, and do not have the same number of free parameters. Therefore a comparison of the likelihoods for either being closer to the ‘true’ model must be based on model selection tools.

Several information criteria commonly used in cosmology (see, e.g., Melia & Maier 2013, and references cited therein) include the Akaike Information Criterion,  $\text{AIC} \equiv -2 \ln L + 2n$ , where  $L$  is the maximum likelihood,  $n$  is the number of free parameters (Liddle 2007), the Kullback Information Criterion,  $\text{KIC} = -2 \ln L + 3n$  (Cavanaugh et al. 2004), and the Bayes Information Criterion,  $\text{BIC} = -2 \ln L + (\ln N)n$ , where  $N$  is the number of data points (Schwarz et al. 1978). With  $\text{AIC}_\alpha$  characterizing model  $\mathcal{M}_\alpha$ , the unnormalized

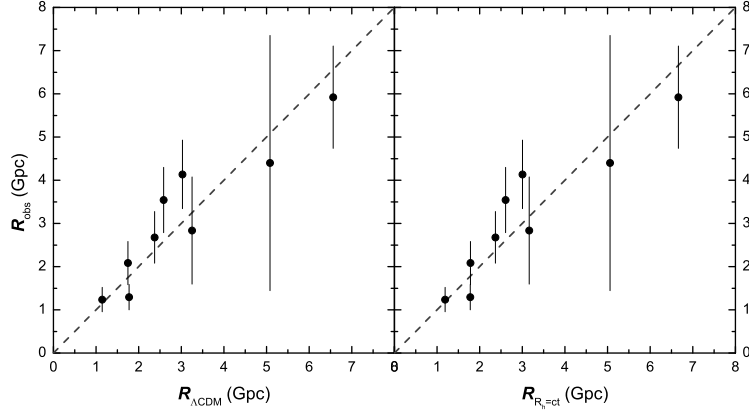


Fig. 2.— Same as Figure 1, except now for the reduced sample of 9 lens systems. The optimized  $\Lambda$ CDM model has  $H_0 = 69^{+12}_{-11}$  km s $^{-1}$  Mpc $^{-1}$ ,  $\Omega_m = 0.51^{+0.32}_{-0.27}$  and  $\eta = 0.19^{+0.16}_{-0.07}$ . The optimized  $R_h = ct$  Universe has  $H_0 = 65^{+13}_{-8.8}$  km s $^{-1}$  Mpc $^{-1}$  and  $\eta = 0.19^{+0.16}_{-0.08}$ .

confidence that this model is true is the Akaike weight  $\exp(-\text{AIC}_\alpha/2)$ . Model  $\mathcal{M}_\alpha$  has likelihood

$$P(\mathcal{M}_\alpha) = \frac{\exp(-\text{AIC}_\alpha/2)}{\exp(-\text{AIC}_1/2) + \exp(-\text{AIC}_2/2)} \quad (11)$$

of being the correct choice in this one-on-one comparison. Thus, the difference  $\Delta\text{AIC} \equiv \text{AIC}_2 - \text{AIC}_1$  determines the extent to which  $\mathcal{M}_1$  is favoured over  $\mathcal{M}_2$ . For Kullback and Bayes, the likelihoods are defined analogously. For the two optimized fits discussed above, the magnitude of the difference  $\Delta\text{AIC} = \text{AIC}_2 - \text{AIC}_1 = 1.7$ , indicates that  $\mathcal{M}_1$  is to be preferred over  $\mathcal{M}_2$ . According to Equation (11), the likelihood of  $R_h = ct$  (i.e.  $\mathcal{M}_1$ ) being the correct choice is  $P(\mathcal{M}_1) \approx 70\%$ . For  $\Lambda$ CDM (i.e.  $\mathcal{M}_2$ ), the corresponding value is  $P(\mathcal{M}_2) \approx 30\%$ . With the alternatives KIC and BIC, the magnitude of the differences  $\Delta\text{KIC} = \text{KIC}_2 - \text{KIC}_1 = 2.7$  and  $\Delta\text{BIC} = \text{BIC}_2 - \text{BIC}_1 = 2.2$ , indicates that  $R_h = ct$  is favored over  $\Lambda$ CDM by a likelihood of  $\approx 75\% - 80\%$  versus  $20\% - 25\%$ .

We also carried out a one-on-one comparison using the reduced sample of only 9 two-image lens systems. In this case, the best  $\Lambda$ CDM fit has a maximum likelihood for

$H_0 = 69_{-11}^{+12}$  ( $1\sigma$ )  $\text{km s}^{-1} \text{Mpc}^{-1}$ ,  $\Omega_m = 0.51_{-0.27}^{+0.32}$  ( $1\sigma$ ) and  $\eta = 0.19_{-0.07}^{+0.16}$  ( $1\sigma$ ). For  $R_h = ct$ , the best fit corresponds to  $H_0 = 65_{-8.8}^{+13}$  ( $1\sigma$ )  $\text{km s}^{-1} \text{Mpc}^{-1}$  and  $\eta = 0.19_{-0.08}^{+0.16}$  ( $1\sigma$ ). Figure 2 is similar to Figure 1, except now for the reduced sample of 9 lenses. In this case, the magnitude of the differences  $\Delta\text{AIC} = 2.0$ ,  $\Delta\text{KIC} = 3.0$ , and  $\Delta\text{BIC} = 2.2$ , indicates that  $R_h = ct$  is preferred over  $\Lambda\text{CDM}$  with a likelihood of  $\approx 73\%$  versus  $\approx 27\%$  using AIC,  $\approx 82\%$  versus  $\approx 18\%$  using KIC, and  $\approx 75\%$  versus  $\approx 25\%$  using BIC.

## 5. Monte Carlo Simulations with a Synthetic Sample

Our results in this paper have shown that time-delay lenses can in fact be used to select one model over another in a one-on-one comparison. But though the likelihood of  $R_h = ct$  being closer to the correct cosmology than  $\Lambda\text{CDM}$  is  $\sim 80\%$  or higher, depending on the choice of information criterion, the outcome  $\Delta \equiv \text{AIC}_1 - \text{AIC}_2$  (and analogously for KIC and BIC) is judged ‘positive’ in the range  $\Delta = 2 - 6$ , and ‘strong’ for  $\Delta > 6$ . The constraints based on the currently known 12 lens systems should therefore be characterized as ‘positive,’ though not yet strong. In this section, we will estimate the sample size required to significantly strengthen the evidence in favor of  $R_h = ct$  or  $\Lambda\text{CDM}$ , by conservatively seeking an outcome even beyond  $\Delta = 6$ , i.e., we will see what is required to produce a likelihood  $\sim 99.7\%$  versus  $\sim 0.3\%$ , corresponding to  $3\sigma$ .

We will consider two cases: one in which the background cosmology is assumed to be  $\Lambda\text{CDM}$ , and a second in which it is  $R_h = ct$ , and we will attempt to estimate the number of time-delay lenses required in each case in order to rule out the alternative (incorrect) model at a  $\sim 99.7\%$  confidence level. The synthetic time-delay lenses are each characterized by a set of parameters denoted as  $(z_l, z_s, \Delta t, \Theta)$ , where  $\Theta \equiv \theta_B^2 - \theta_A^2$ , and are generated using the following procedure:

1. Since the 12 observed lens redshifts all fall in the range  $0.26 \leq z_l \leq 0.89$ , and the source redshifts are  $1.246 \leq z_s \leq 2.719$ , with a time delay  $-150 \leq \Delta t \leq 150$  (days), we assign  $z_l$  uniformly between 0.2 and 1.0,  $z_s$  uniformly between 1.2 and 3.0, and  $\Delta t$  uniformly between  $-150$  and  $150$  days.

2. We first infer  $\Theta \equiv (\theta_B^2 - \theta_A^2)$  from Equation 4 corresponding either to the  $R_h = ct$  Universe with  $H_0 = 70 \text{ km s}^{-1} \text{ Mpc}^{-1}$  (§ 5.1), or to  $\Lambda$ CDM with  $\Omega_m = 0.3$ ,  $\Omega_\Lambda = 0.7$  and  $H_0 = 70 \text{ km s}^{-1} \text{ Mpc}^{-1}$  (§ 5.2). We then assign a random deviation ( $\Delta\Theta$ ) to the  $\Theta$  value within the  $3\sigma$  confidence interval, i.e., we put  $\Theta' = \Theta + (2x - 1) \cdot 3\sigma$ , where  $x$  is a uniform random variable between 0 and 1, and  $\sigma = 0.04 \Theta$ . This value of  $\sigma$  is taken from the current observed sample, which shows a median deviation  $\sim 0.04 \Theta$ . The same relative error is assigned to  $\Theta'$ .

3. Since the observed  $\sigma_{\Delta t}$  is about 4% of  $\Delta t$ , we will also assign dispersion  $\sigma_{\Delta t} = 0.04 \Delta t$  to the synthetic sample.

This sequence of steps is repeated for each lens system in the sample, which is enlarged until the likelihood criterion discussed above is reached. As with the real 12-lens sample, we optimize the model fits by maximizing the joint likelihood function in equation (7). We employ Markov-chain Monte Carlo techniques. In each Markov chain, we generate  $10^5$  samples according to the likelihood function. Then we derive the coefficients  $\eta$  and the cosmological parameters from a statistical analysis of the sample.

### 5.1. Assuming $R_h = ct$ as the Background Cosmology

We have found that a sample of at least 1,000 time-delay lenses is required in order to rule out  $\Lambda$ CDM at the  $\sim 99.7\%$  confidence level. The optimized parameters corresponding to the best-fit  $\Lambda$ CDM model for these simulated data are displayed in figure 3. To allow

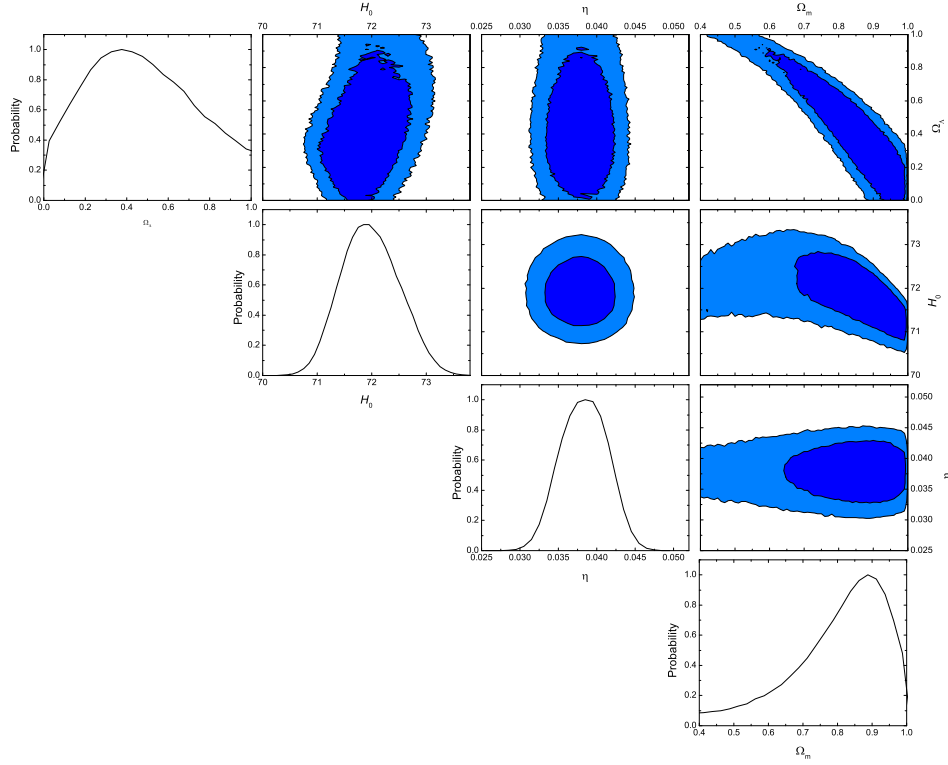


Fig. 3.— The 1-D probability distributions and 2-D regions with the  $1\sigma$  and  $2\sigma$  contours corresponding to the parameters  $\Omega_m$ ,  $\Omega_\Lambda$ ,  $H_0$ , and  $\eta$  in the best-fit  $\Lambda$ CDM model, using the simulated sample with 1,000 lens systems, assuming  $R_h = ct$  as the background cosmology.

for the greatest flexibility in this fit, we relax the assumption of flatness, and allow  $\Omega_\Lambda$  to be a free parameter, along with  $\Omega_m$ . Figure 3 shows the 1-D probability distribution for each parameter ( $\Omega_m$ ,  $\Omega_\Lambda$ ,  $H_0$ ,  $\eta$ ), and 2-D plots of the  $1\sigma$  and  $2\sigma$  confidence regions for two-parameter combinations. The best-fit values for  $\Lambda$ CDM using the simulated sample with 1,000 lens systems in the  $R_h = ct$  Universe are  $\Omega_m = 0.85^{+0.21}_{-0.21}$  ( $1\sigma$ ),  $\Omega_\Lambda = 0.48^{+0.47}_{-0.48}$ ,  $H_0 = 72^{+0.81}_{-0.80}$  ( $1\sigma$ ) km s<sup>-1</sup> Mpc<sup>-1</sup>, and  $\eta = 0.038^{+0.0040}_{-0.0050}$  ( $1\sigma$ ).

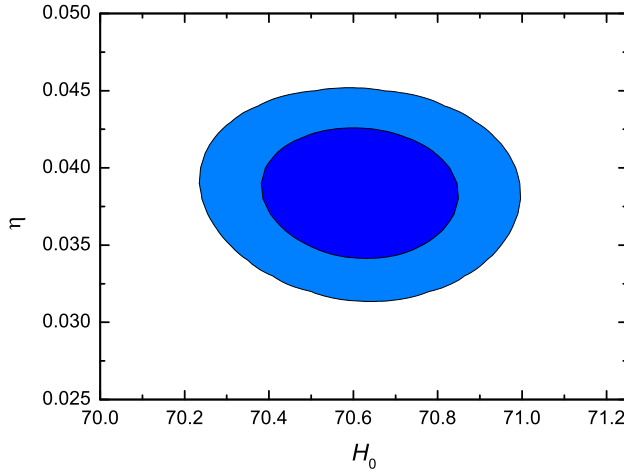


Fig. 4.— The 2-D region with the  $1\sigma$  and  $2\sigma$  contours for the parameters  $H_0$  and  $\eta$  in the  $R_h = ct$  Universe, using a sample of 1,000 time-delay lenses, simulated with  $R_h = ct$  as the background cosmology. The assumed value for  $H_0$  in the simulation was  $H_0 = 70$  km s<sup>-1</sup> Mpc<sup>-1</sup>.

In figure 4, we show the corresponding 2-D contours in the  $H_0 - \eta$  plane for the  $R_h = ct$  Universe. The best-fit values for the simulated sample are  $H_0 = 71^{+0.24}_{-0.24}$  ( $1\sigma$ ) km s<sup>-1</sup> Mpc<sup>-1</sup> and  $\eta = 0.038^{+0.0050}_{-0.0040}$  ( $1\sigma$ ).

Since the number  $N$  of data points in the sample is now much greater than one, the most appropriate information criterion to use is the BIC. The logarithmic penalty in this model selection tool strongly suppresses overfitting if  $N$  is large (the situation we have



here, which is deep in the asymptotic regime). With  $N = 1,000$ , our analysis of the simulated sample shows that the BIC would favor the  $R_h = ct$  Universe over  $\Lambda$ CDM by an overwhelming likelihood of 99.7% versus only 0.3% (i.e., the prescribed  $3\sigma$  confidence limit).

## 5.2. Assuming $\Lambda$ CDM as the Background Cosmology

In this case, we assume that the background cosmology is  $\Lambda$ CDM, and seek the minimum sample size to rule out  $R_h = ct$  at the  $3\sigma$  confidence level. We have found that a minimum of 135 time-delay lenses are required to achieve this goal. To allow for the greatest flexibility in the  $\Lambda$ CDM fit, here too we relax the assumption of flatness, and allow  $\Omega_\Lambda$  to be a free parameter, along with  $\Omega_m$ . In figure 5, we show the 1-D probability distribution for each parameter ( $\Omega_m$ ,  $\Omega_\Lambda$ ,  $H_0$ ,  $\eta$ ), and 2-D plots of the  $1\sigma$  and  $2\sigma$  confidence regions for two-parameter combinations. The best-fit values for  $\Lambda$ CDM using this simulated sample with 135 lens systems are  $\Omega_m = 0.34^{+0.20}_{-0.18}$  ( $1\sigma$ ),  $\Omega_\Lambda = 0.58$ ,  $H_0 = 71^{+2.1}_{-2.1}$  ( $1\sigma$ )  $\text{km s}^{-1} \text{Mpc}^{-1}$ , and  $\eta = 0.041^{+0.011}_{-0.013}$  ( $1\sigma$ ). Note that the simulated lenses give a good constraint on  $\Omega_m$ , but a weak one on  $\Omega_\Lambda$ ; only an upper limit of 0.90 can be set at the  $1\sigma$  confidence level.

The corresponding 2-D contours in the  $H_0 - \eta$  plane for the  $R_h = ct$  Universe are shown in figure 6. The best-fit values for the simulated sample are  $H_0 = 65^{+0.57}_{-0.63}$  ( $1\sigma$ )  $\text{km s}^{-1} \text{Mpc}^{-1}$  and  $\eta = 0.048^{+0.011}_{-0.011}$  ( $1\sigma$ ). These are similar to those in the standard model, but not exactly the same, reaffirming the importance of reducing the data separately for each model being tested. With  $N = 135$ , our analysis of the simulated sample shows that in this case the BIC would favor  $\Lambda$ CDM over  $R_h = ct$  by an overwhelming likelihood of 99.7% versus only 0.3% (i.e., the prescribed  $3\sigma$  confidence limit).

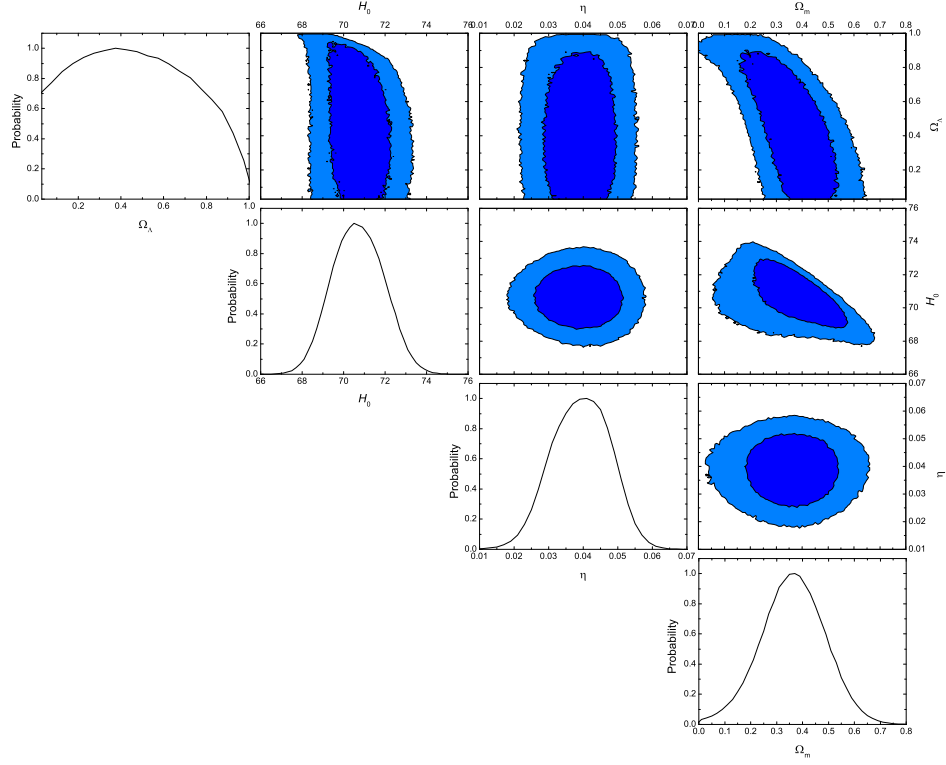


Fig. 5.— Same as Figure 3, except now with  $\Lambda$ CDM as the (assumed) background cosmology. The simulated model parameters were  $\Omega_m = 0.3$ ,  $\Omega_\Lambda = 0.7$  and  $H_0 = 70 \text{ km s}^{-1} \text{ Mpc}^{-1}$ .

## 6. Conclusions

The general agreement between theory and observation displayed in Figures 1 and 2 is promising, particularly since this work was based on the use of a single isothermal sphere profile for the lens mass distribution. It would be helpful to have additional information from which one may extract the lens structure from individual images. Up to now, these approaches have been used to optimize parameters in  $\Lambda$ CDM itself, but not for an actual one-on-one comparison between competing cosmological models. This must be done because the results we have presented here already indicate a strong likelihood of being able to discriminate between models such as  $\Lambda$ CDM and  $R_h = ct$ . Such comparisons have already been made using, e.g., cosmic chronometers (Melia & Maier 2013), gamma-ray bursts (Wei et al. 2013), and Type Ia SNe (Wei et al. 2014). The use of time-delay lenses introduces yet another standard ruler, with systematics different from those encountered elsewhere, thus providing an invaluable tool with which to cross-check the outcomes of these other important tests.

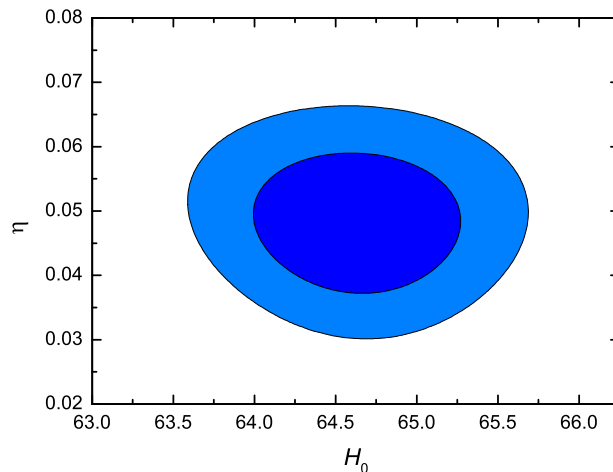


Fig. 6.— Same as Figure 4, except now with  $\Lambda$ CDM as the (assumed) background cosmology.

But though time-delay lens observations currently tend to favor  $R_h = ct$  over  $\Lambda$ CDM,

the known sample of such systems is still too small for us to completely rule out either model. We have therefore considered two synthetic samples with characteristics similar to those of the 12 known systems, one based on a  $\Lambda$ CDM background cosmology, the other on  $R_h = ct$ . From the analysis of these simulated lenses, we have estimated that a sample of about 150 lenses would be needed to rule out  $R_h = ct$  at a  $\sim 99.7\%$  confidence level if the real cosmology is in fact  $\Lambda$ CDM, while a sample of at least 1,000 systems would be needed to similarly rule out  $\Lambda$ CDM if the background cosmology were instead  $R_h = ct$ . The difference in required sample size results from  $\Lambda$ CDM’s greater flexibility in fitting the data, since it has a larger number of free parameters. Such a level of accuracy may be achievable with the successful implementation of surveys, such as DES, VST ATLAS, and LSST.

We gratefully acknowledge helpful discussions with Gary Bernstein concerning the Dark Energy Survey’s expected image quality, and we thank the anonymous referee for important suggestions to greatly improve this manuscript. This work is partially supported by the National Basic Research Program (“973” Program) of China (Grants 2014CB845800 and 2013CB834900), the National Natural Science Foundation of China (grants Nos. 11322328 and 11373068), the One-Hundred-Talents Program, the Youth Innovation Promotion Association, and the Strategic Priority Research Program “The Emergence of Cosmological Structures” (Grant No. XDB090000000) of the Chinese Academy of Sciences, and the Natural Science Foundation of Jiangsu Province. F.M. is grateful to Amherst College for its support through a John Woodruff Simpson Lectureship, and to Purple Mountain Observatory in Nanjing, China, for its hospitality while part of this work was being carried out. This work was partially supported by grant 2012T1J0011 from The Chinese Academy of Sciences Visiting Professorships for Senior International Scientists, and grant GDJ20120491013 from the Chinese State Administration of Foreign Experts Affairs.

Table 1. Time Delay (Two-image) Lenses

System	$z_l$	$z_s$	$\theta_A$ (arcsec)	$\theta_B$ (arcsec)	$\Delta t = t_A - t_B$ (days)	$\mathcal{R}_{\text{obs}}$ (Gpc)	$\mathcal{R}_{\Lambda\text{CDM}}$ (Gpc)	$\mathcal{R}_{R_h=ct}$ (Gpc)	Refs.
B0218+357	0.685	0.944	$0.057 \pm 0.004$	$0.280 \pm 0.008$	$+10.5 \pm 0.2$	$5.922 \pm 1.757$	5.268	5.361	1–3
B1600+434	0.414	1.589	$1.14 \pm 0.075$	$0.25 \pm 0.074$	$-51.0 \pm 2.0$	$2.082 \pm 0.677$	1.403	1.435	4,5
FBQ0951+2635	0.26	1.246	$0.886 \pm 0.004$	$0.228 \pm 0.008$	$-16.0 \pm 2.0$	$1.237 \pm 0.391$	0.917	0.956	6
HE1104-1805	0.729	2.319	$1.099 \pm 0.004$	$2.095 \pm 0.008$	$152.2 \pm 3.0$	$1.976 \pm 0.575$	2.202	2.170	2,7,8
HE2149-2745	0.603	2.033	$1.354 \pm 0.008$	$0.344 \pm 0.012$	$-103.0 \pm 12.0$	$2.676 \pm 0.837$	1.909	1.908	6,9
PKS1830-211	0.89	2.507	$0.67 \pm 0.08$	$0.32 \pm 0.08$	$-26 \pm 5$	$2.835 \pm 1.385$	2.620	2.546	10,11
Q0142-100	0.49	2.719	$1.855 \pm 0.002$	$0.383 \pm 0.005$	$-89 \pm 11$	$1.295 \pm 0.408$	1.428	1.431	6,12
Q0957+561	0.36	1.413	$5.220 \pm 0.006$	$1.036 \pm 0.11$	$-417.09 \pm 0.07$	$0.837 \pm 0.243$	1.256	1.294	6, 13,14
SBS 0909+532	0.83	1.377	$0.415 \pm 0.126$	$0.756 \pm 0.152$	$+45.0 \pm 5.5$	$4.398 \pm 3.107$	4.085	4.072	6,15
SBS 1520+530	0.717	1.855	$1.207 \pm 0.004$	$0.386 \pm 0.008$	$-130.0 \pm 3.0$	$4.135 \pm 1.203$	2.435	2.419	6,16
SDSS J1206+4332	0.748	1.789	$1.870 \pm 0.088$	$1.278 \pm 0.097$	$-116 \pm 5$	$2.543 \pm 0.934$	2.632	2.612	17
SDSS J1650+4251	0.577	1.547	$0.872 \pm 0.027$	$0.357 \pm 0.042$	$-49.5 \pm 1.9$	$3.542 \pm 1.082$	2.079	2.098	6,18

*References:* (1) Carilli et al. (1993); (2) Lehár et al. (2000); (3) Wucknitz et al. (2004); (4) Jackson et al. (1995); (5) Dai & Kochanek (2005); (6) Kochanek et al. (2008); (7) Wisotzki et al. (1993); (8) Poindexter et al. (2007); (9) Burud et al. (2002); (10) Lovell et al. (1998); (11) Meylan et al. (2005); (12) Koptelova et al. (2012); (13) Falco et al. (1997); (14) Colley et al. (2003); (15) Dai & Kochanek (2009); (16) Auger et al. (2008); (17) Paraficz et al. (2009); (18) Vuissoz et al. (2007).

## REFERENCES

- Auger, M. W., Fassnacht, C. D., Wong, K. C., Thompson, D., Matthews, K. & Soifer, B. T. 2008, *ApJ*, 673, 778
- Balmès, I. & Corasaniti, P. S. 2013, *MNRAS*, 431, 1528
- Banerji, M., Abdalla, F., Lahav, O. & Lin, H. 2008, *MNRAS*, 386, 1219
- Bernstein, G. 2014, private communication
- Blandford, R. & Narayan, R. 1986, *ApJ*, 310, 568
- Blandford, R. D., Oguri, M., Marshall, P., Baltz, E. A., Bradac, M., Fassnacht, C. D. & LSST Collaboration 2006, AAS Meeting 209, No. 86.12
- Bradac M., Allen, S. W., Treu, T., Ebeling, H., Massey, R., Morris, R. G., von der Linden, A. & Applegate, D. 2008, *ApJ*, 687, 959
- Buckley-Geer, E. J., Dark Energy Survey Collaboration 2014, AAS Meeting 223, No. 248.01
- Burud, I. et al. 2002, *A&A*, 383, 71
- Cao, S., Pan, Y., Biesiada, M., Godlowski, W. & Zhu, Z.-H. 2012, *JCAP*, issue 3, id. 16
- Carilli, C. L., Rupen, M. P. & Yanny, B. 1993, *ApJ*, 412, L59
- Cavanaugh, J. E. 2004, *Aust. N. Z. J. Stat.*, 46, 257
- Chang, C., Jarvis, M., Jain, B., Kahn, S. M., Kirkby, D., Connolly, A., Krughoff, S., Peng, E.-H. & Peterson, J. R. 2014, *MNRAS*, 434, 2121
- Coles, J. 2008, *ApJ*, 679, 17
- Colley, W. N. et al. 2003, *ApJ*, 587, 71

- Dai, X. & Kochanek, C. S. 2005, *ApJ*, 625, 633
- Dai, X. & Kochanek, C. S. 2009, *ApJ*, 692, 667
- Eigenbrod, A., Courbin, F., Vuissoz, C., Meylan, G., Saha, P. & Dye, S. 2005, *A&A*, 436, 25
- Falco, E. E., Shapiro, I. I., Moustakas, Leonidas A. & Davis, M. 1997, *ApJ*, 484, 70
- Guimaraes, A.C.C. & Sodré, L. Jr. 2009, *Highlights of Astronomy*, 15, 75
- Hewett, P. C. & Wild, V. 2010, *MNRAS*, 405, 2302
- Jackson, N. et al. 1995, *MNRAS*, 274, L25
- Jean, C., Claeskens, J.-F. & Surdej, J. 2001, *Gravitational Lensing: Recent Progress and Future Goals*, ASP Conference Proceedings, Vol. 237. Ed. T. G. Brainerd and C. S. Kochanek (ASP: San Francisco)
- Keeton, C. R., Gaudi, B. S. & Petters, A. O. 2003, *ApJ*, 598, 138
- Kochanek, C. S., Falco, E. E., Impey, C., Lehár, J., McLeod, B. & Rix, H.-W. 2008, available at <http://www.cfa.harvard.edu/castles/>
- Koopmans, L.V.E. et al. 2009, *ApJ*, 703, L51
- Koposov, S. E., Irwin, M., Belokurov, V., Gonzales-Solares, E., Kupcu-Yoldas, A., Lewis, J., Metcalfe, N. and Schanks, T. 2014, *MNRAS Letters*, submitted (arXiv:1403.3409)
- Koptelova, E. et al. 2012, *A&A*, 544, A51
- Lehár, J. et al. 2000, *ApJ*, 536, 584
- Liddle, A. R. 2007, *MNRAS*, 377, L74

- Lovell, J.E.J., Jauncey, D. L., Reynolds, J. E., Wieringa, M. H., King, E. A., Tzioumis, A. K., McCulloch, P. M. & Edwards, P. G. 1998, *ApJ*, 508, L51
- Marshall, P. J., Sandford, C. P., Fassnacht, C. D., Meldgin, D. R., Oguri, M., Suyu, S. H., Auger, M. W., LSST Strong Lensing Science Collaboration 2011, AAS Meeting 217, No. 252.22
- Melia, F. 2007, *MNRAS*, 382, 1917
- Melia, F. 2013, *ApJ*, 764, 72
- Melia, F. & Maier, R. S. 2013, *MNRAS*, 432, 2669
- Melia, F., & Shevchuk, A. S. H. 2012, *MNRAS*, 419, 2579
- Meylan, G., Courbin, F., Lidman, C., Kneib, J.-P. & Tacconi-Garman, L. E. 2005, *A&A*, 438, L37
- Oguri, M., Taruya, A., Suto, Y. & Turner, E. L. 2002, *ApJ*, 568, 488
- Oguri, M. 2007, *ApJ*, 660, 1
- Oguri, M., & Marshall, P. J. 2010, *MNRAS*, 405, 2579
- Paraficz, D. & Hjorth, J. 2009, *A&A Letters*, 507, L49
- Paraficz, D. & Hjorth, J. 2010, *ApJ*, 712, 1378
- Petters, A. O., Levine, H., & Wambsganss, J. 2001, *Singularity theory and gravitational lensing* / Arlie O. Petters, Harold Levine, Joachim Wambsganss. Boston : Birkhäuser, c2001. (Progress in mathematical physics ; v. 21),
- Poindexter, S., Morgan, N., Kochanek, C. S. & Falco, E. E. 2007, *ApJ*, 660, 146
- Refsdal, S. 1964, *MNRAS*, 128, 307



- Rusin, D., Kochanek, C. S. & Keeton, C. R. 2003, ApJ, 595, 29
- Sagar, R., Kumar, B. & Omar, A. 2013, arXiv:1304.0235
- Schneider, P., Kochanek, C. & Wambsgness, J. 2006, in *Gravitational Lensing: Strong, Weak, and Micro: Saas-Fee Advanced Course*, eds. Meylan, G., Jetzer, P. & North, P. (Springer: Berlin)
- Schneider, M. D. 2014, PRL, 112, id.061301
- Schwarz, G. 1978, Ann. Statist., 6, 461
- Suyu, S. H., Marshall, P. J., Auger, M. W., et al. 2010, ApJ, 711, 201
- Suyu, S. H. et al. 2013, ApJ, 766, 70
- Treu, T. & Koopmans, L.V.E. 2002, MNRAS Letters, 337, L6
- Treu, T., Koopmans, L. V., Bolton, A. S., Burles, S., & Moustakas, L. A. 2006, ApJ, 640, 662
- Tyson, T., Wittman, D., Hennawi, J. & Spergel, D. 2002, American Physical Society, April Meeting ID: APR02, abstract No. Y6.004
- Vegetti, S., Koopmans, L.V.E., Bolton, A., Treu, T. & Gavazzi, R. 2010, MNRAS, 408, 1969
- Vuissoz, C., Courbin, F., Sluse, D., Meylan, G., Ibrahimov, M., Asfandiyarov, I., Stoops, E., Eigenbrod, A., Le Guillou, L., van Winckel, H. & Magain, P. 2007, A&A, 464, 845
- Warren, S. J., & Dye, S. 2003, ApJ, 590, 673
- Wei, J.-J., Wu, X. & Melia, F. 2013, ApJ, 772, 43
- Wei, J.-J., Wu, X. & Melia, F. 2014, ApJ, submitted

White, R. L. et al. 2000, ApJS, 126, 133

Wucknitz, O., Biggs, A. D. & Browne, I.W.A. 2004, MNRAS, 349, 14

Wisotzki, L., Koehler, T., Kayser, R. & Reimers, D. 1993, A&A, 278, L15

Witt, H. J., Mao, S. & Keeton, C. R. 2000, ApJ, 544, 98

York, T., Jackson, N., Browne, I.W.A., Wucknitz, O. & Skelton, J. E. 2005, MNRAS, 357,  
124